UV LED Excited Time-Gated Luminescence Flow Cytometry: Evaluation For Rare-Event Particle Counting

Dayong Jin[1*], Belinda Ferrari[2], Robert Leif[3*], Sean Yang[3] Lidia M. Vallarino[4], John Williams[4], and James Piper[1]

[1]Centre for Lasers & Applications, Division of Information & Communication Sciences, Macquarie University, NSW 2109 Australia

[2] Environmental Biotechnology CRC and Biotechnology Research Institute, Macquarie University, NSW 2109 Australia

[3] Newport Instruments, 5648 Toyon Road, San Diego, CA, USA 92115-1022

[4] Department of Chemistry, Virginia Commonwealth University, 1001 W. Main St., Box 2006, Richmond, VA USA 23284-2006

ABSTRACT

Flow cytometric detection of specific rare-event targets within high-background samples such as water or food are frequently defeated by the extremely large population of non-target background particles. Time-gated detection of long lifetime fluorescence (>10μs) labeled microbial targets has been proven highly efficient in suppressing this non-target autofluorescent (<0.1μs) background. A time-gated luminescence (TGL) flow cytometer using UV LED excitation has demonstrated the successful detection of rare-event particles in high autofluorescence background samples. In this report, high-quality 5μm europium beads were made (homogenous intensity and aggregation free) for a detailed evaluation of the prototype performance. The known number of beads (10±2, 100±20 and 1000±100) were first sorted by a conventional flow cytometry sorter, and spiked into an environmental water concentrate (1 ml; containing >10 million non-target particles). The recovery rate for counting these very-rare-event particles using the TGL flow cytometer was then found to be 100%±20% between bead concentrations evaluated.

Key words: flow cytometry, true positive, rare event, europium, time-gated luminescence, UV LED, autofluorescence

INTRODUCTION

Specific and accurate detection of rare-event micron-sized targets in a rapid and cost-effective fashion is both important and challenging for the clinical[1-3] and environmental fields [4,5]. A rare event can be defined as one that occurs at a frequency of less than 1:10, 000[3], and most of challenging biological and clinical applications requires accurate target cell detection against non-target cells at a frequency of less than 1: 1000,000: for example, in the field of noninvasive prenatal diagnosis, fetal nucleated red blood cells (NRBCs) are present in maternal blood at frequencies as low as $1/10^4$-$1/10^9$ nucleated maternal cells[6], and in the field of water safety inspection, due to the very low infectious dose of some waterborne pathogens, analysis methods need to be sufficiently sensitive to detect a single microorganism (e.g. *Cryptosporidium parvum* and *Giardia lamblia*) in as much as 100 L water containing millions of non-target microorganisms and particles[7].

* send all correspondence to: Dr. Dayong Jin, jin@ics.mq.edu.au, phone 61 2 9850 4168; except questions about the calibration beads should be sent to Dr. Robert Leif, rleif@rleif.com, phone 1 619 582-0437, fax 1 619 501-1953

Imaging, Manipulation, and Analysis of Biomolecules, Cells, and Tissues VI,
edited by Daniel L. Farkas, Dan V. Nicolau, Robert C. Leif,
Proc. of SPIE Vol. 6859, 68590O, (2008) · 1605-7422/08/$18 · doi: 10.1117/12.762077

Microscopic quantification methods are laborious, often requiring skilled personal[6]. Flow cytometry has been shown to be a successful alternative for the quantification of microbial cells from within complex samples such as pathogens in water [8], beverages[9], and milk[10] with the prospect in the future of rapid real-time analysis [2,7,11]. The accurate detection of target microorganisms from within an intrinsically fluorescent matrix of non-target particles such as minerals, plant debris and algae, often requires multi-color fluorescence staining followed by multi-spectrum detection techniques[4,12]. The high sensitivity and specificity required for these applications means that detection is often hampered, leading to flow cytometric reporting of false positives, particularly when the target organism is present in low numbers .

We previously reported a practical flow cytometry method based on time-gated detection of long-lifetime luminescence labeled targets [13,14]. In these studies, time-gated detection of target events in temporal, spectral and spatial 3-D domains rendered both the scattering and autofluorescence backgrounds invisible. This enhanced the detection likelihood for the low concentration of micron-size targets. Our early development of time-gated luminescence (TGL) flow cytometry technique focused on a continuous-flow-section approach using LED excitation [13,14]. This technique showed great potential for the detection of trace amounts of micron-sized targets by flow cytometry. However, these studies were limited by the lack of long lifetime fluorescent calibration beads, and a number of experimental issues, such as obtaining particle counts, a histogram of the distribution of particle luminescent intensities and the determination of rare-event recovery frequencies were not feasible. In this report, a prototype lot of 5µm europium-labelled beads which display long-lived (>~340µs) fluorescence were utilized to evaluate the performance of TGL flow cytometry, specifically focusing on rare-event recovery capabilities in environmental samples.

MATERIALS AND METHODS

Time-gated luminescence flow cytometer

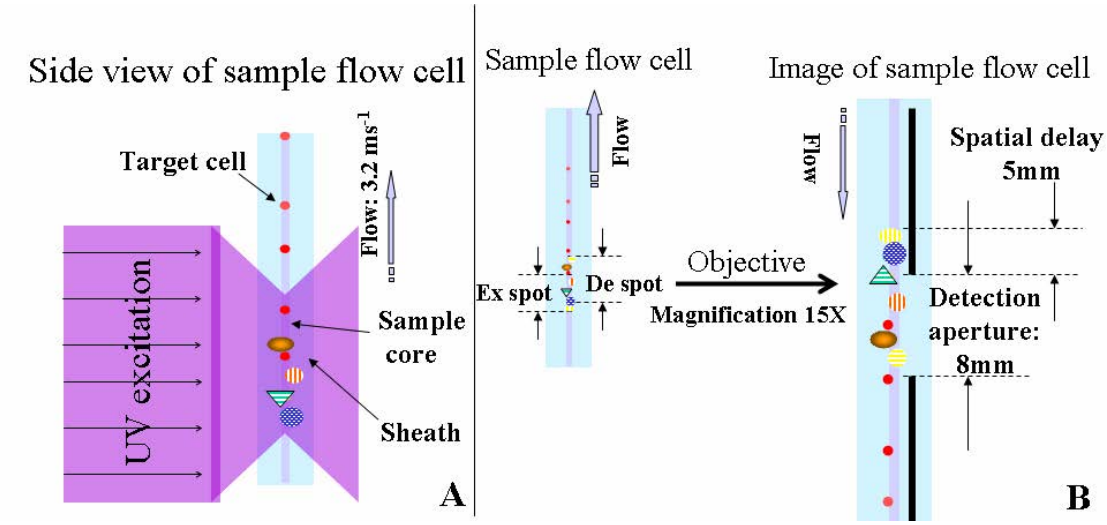

Figure 1. Geometry schematic layout of TGL flow cytometer: A). UV LED excitation at flow cell: in the sample flow stream, the round solid particles represent target europium particles/cells and the other larger round (pattern), oval and triangle particles represent non-target autofluorescence particles/cells; B). spatial delayed detection at image plane.

The details on both concepts and prototype operation of TGL flow cytometer were stated previously [13,14]. Briefly, Figure 1 shows the basics of geometric layout for the current development of TGL flow cytometer: The targets of interest are fluorescently labeled with a long-lived fluorescent probe, typically lanthanide complexes, and then excited with a pulsed LED (pulse duration of up to 100 μs) as they flow in single cell profile through the hydrodynamically focused laminar stream (figure 1A). Once the excitation pulse has extinguished, the autofluorescence fades rapidly (within 0.1 μs). In the mean time, signal luminescence from targets loses little of their original intensity and continues to luminance as it progresses downstream from the excitation interrogation spot. The implementation of periodically pulsed illumination and time-delayed gates have been carefully designed to achieve 100% spatial detection of TGL particles (figure 1B). This takes account of flow speed, illumination, detection apertures, fluorescence label lifetime, pulsed illumination and gated-detection-timing sequences.

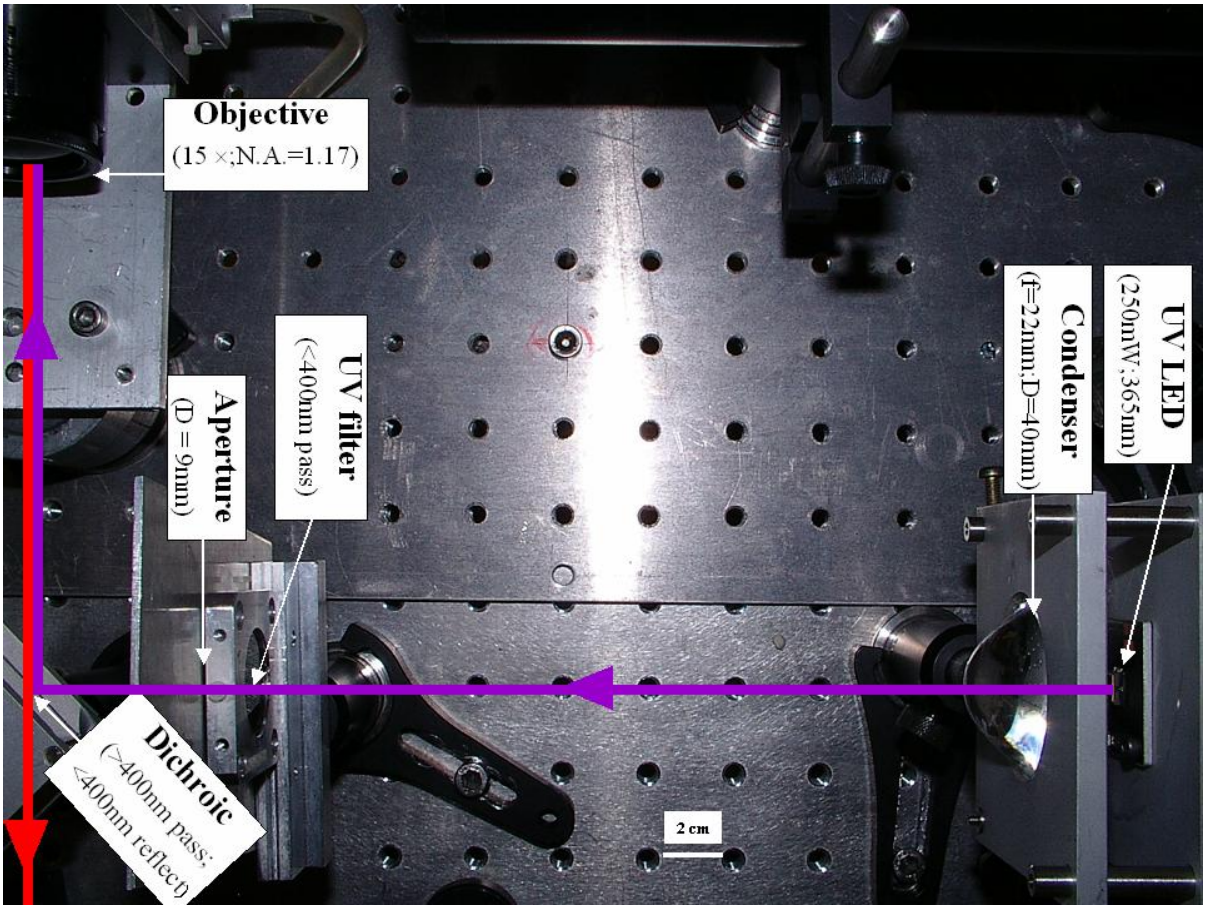

Figure 2 Layout of the UV LED excitation system applying epi-illumination optics to excite the time-gated luminescence flow cytometer.

Figure 2 shows the optical layout of the UV LED excited TGL flow cytometer: The high intensity UV LED (maximum CW output power of 250mW at 365nm, NCCU033A; Nichia Corp. Japan) is mounted on aluminum plate which provides improved heat dissipation. The light at a large solid angle (>45^0C) is collected by a high N.A. condenser lens with the image of the LED is projected on the excitation aperture plane after a UV excitation filter; the approximately parallel beam is then reflected by the dichroic mirror and redirected into the flow cell objective. The TGL repetition rate was 6.45 k Hz with excitation pulses of 100 μs duration followed by a ~10 μs time-resolving period and ~45 μs gated-detection period. The average flow velocity was

calibrated as 3.2 m s^{-1} (sample flow rate: 100µl per minute). The UV LED was focused generating a $(530\mu m)^2$ illumination spot with ~ 15mW peak power on the sample stream, and the CPMT (channel photomultiplier tube) detector operated at photoelectric gain of ~ 2×10^6. The detected anode current from the CPMT was converted into voltage signal by a current-voltage preamplifier (model DHPCA-200, FEMTO, Germany; 400K bandwidth; 10^5 V/A). This signal was subsequently digitized by a 1.25MHz data acquisition card (DAQ) (NI PCI-6251, National Instruments Australia Corp, NSW, Australia) for real-time TGL event counting by programmed software in Labview 7.1 Express (National Instruments Australia Corp, NSW, Australia).

Europium calibration Beads

The prototype Newport Instruments Fire Red™ beads were aqueous suspensions of europium-complex-loaded polymer microspheres (beads), which showed low aggregation. The 5.0-µm-europium microspheres were reasonably uniform in size (Figure 3A). The beads contain Eu^{3+} coordination complexes which have an excitation maximum at approximately 370 nm and emit in a narrow region around 620 nm with luminescence lifetime of 320±30 µs (in water). Before each flow cytometry operation, the sample was ultrasonicated for 4 minutes to remove particle aggregation.

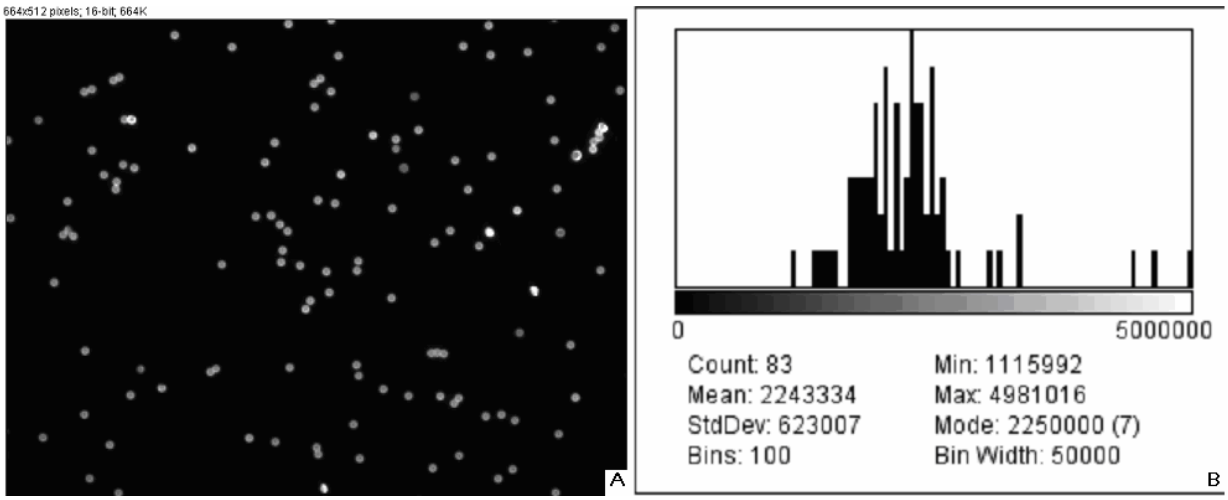

Figure 3 the Newport Instrument's Fire Red 5µm europium calibration beads: A). luminescence image; B). integrated intensity analysis of each individual beads.

TGL microscopy image

The variation of luminescence intensity amongst individual beads was recorded by imaging the luminescence beads under UV LED excitation with a luminescence microscope[15]. Images were obtained with essentially continuous excitation from a Nichia UV LED, Model NCCU033[16]. According to the manufacturer's specifications, the peak wavelength, optical power output, and spectrum half width were 365 nm, 100 mW, and 10 nm, respectively. A Laserlab power-supply (http://www.laserlab.com/) was used to drive the LED in pulsed mode. One millisecond-wide pulses were delivered at 1,000 Hz to power the LED. The LED was positioned [16] close to the back of a Linos condenser (16/21.4 mm) (part no. 06 3010, http://www.linos-photonics.com), which was attached to the excitation entrance of the epi-illuminator of a modified Leitz MPV II fluorescence microscope. The emitted light traversed an Omega Optical (Brattleboro, VT) PloemoPak cube UV DAPI, equipped with a 365 nm narrow-band-width excitation filter (Omega 365HT25) and a 400 nm beam-splitter (Omega 400DCLP02). The optical path of the CCD was equipped with either a 619 nm narrow-band emission filter (Omega 618.6NB5.6). A representative image is shown in Figure 3A. These images have not been corrected for the inhomogeneous illumination provided by the UV LED. In order to calibrate the time-gated luminescence intensity from each particle, the intensities were analysed using "ImageJ" software

(http://rsb.info.nih.gov/ij/). Due to the difficulty in calculating intensities from the overlapping particles, all overlapping particles and partially imaged particles from the original image were omitted. The target europium microspheres showed that the differences between the extremes of the europium dye emission from the individual beads has been substantially improved [maximum/minimum=4.46; and the CV=27.8% (see figure 3B] reduced from the Invitrogen beads in our previous report (maximum/minimum=14.7; CV=103%).

Flow cytometric cell sorting to produce calibration beads

Both europium-labelled and FITC-labelled bead spike samples consisting of 10, 100 or 1000 beads were prepared for recovery determinations using fluorescence activated cell sorting as described previously . Briefly, calibration spikes were prepared using the BD FACSAria™ flow cytometer (BD Biosciences, Macquarie Research Park, Sydney, Australia) in single-cell mode. A gate (R1) was defined around the single beads populations within a bivariate dotplot of SSC versus FSC and events detected in R1 were sorted directly into microfuge or FACS tubes for analysis. Sheath fluid consisted of undiluted Osmosol (Lab Aids Pty Ltd, Narrabeen, NSW, Australia). Each spike calibration set was produced in triplicate for each analysis. The mean and standard deviation of the 10 and 100 bead sets was determined by sorting onto glass slides and confirming numbers by epifluorescence microscopy.

Microscopy confirmation of beads spikes

The number of beads present in the 100 and 10 calibration bead sets were determined by epifluorescence microscopy using an Axioskop 2 microscope (Carl Zeiss, Sydney, Australia) with appropriate filters for the examination of FITC and Europium fluorescence (DAPI filter). For the europium bead preparations, the spike beads sets were 97 ± 1 and 10.3 ± 0.7 for the 100 and 10-bead sample sets respectively. For the FITC bead preparations, the spike beads sets were 101 ± 1 and 9 ± 1 for the 100 and 10-bead sample sets respectively.

Environmental water sample preparation

A large volume of backwash filtered water from a drinking water treatment plant was prepared for use as a quality control sample. Additionally, a 10L water sample was processed using calcium carbonate flocculation modified for 100 ml volumes [17]. Following concentration, the water samples were centrifuged (3,500 x g; 10 minutes) and the supernatant discarded. Prior to use, concentrates were centrifuged (13, 000 x g; 10 minutes) and the supernatant discarded. Samples were resuspended in mAb buffer (to initial volume) and filtered through a 38 μm stainless steel mesh filter (Metal Mesh Pty, Ltd, Sydney) housed within in a swinnex filter unit (Millipore, North Ryde, Australia) using a syringe. The sample was forced through the filter leaving large aggregates behind.

RESULTS

Real-time counting histogram

Figure 4A shows one typical 4-millisecond section (consisted of 26 TGL cycles) of the TGL flow cytometer pulse train. From our previous knowledge[14], we know that under the same operational settings, the real-time observation of signal trains for either pure samples or samples with a large amount of autofluorescence backgrounds showed no difference in terms of background level during the time-gated detection phase. In this test, pure europium calibration beads were tested. The observation shows that the TGL flow counting background level was less than 0.3 volts when no TGL event present in the time-gated detection periods (corresponding to flow-sections which did not contain target beads). With the UV LED switched off, only the CPMT dark count (electronic noise) was occasionally observed (data not shown) during the time-gated detection periods; when increasing the UV LED injection current, the background level was observed to increase and become independent on the LED injection current in the range of 0.2A to 1A. As previously noted [18] on the characteristics of UV LED native emissions, the majority of detection background in the time-gated detection phase was believed from the UV LED native emissions, which were detected by the CPMT

detector, even though, it was shielded by a 610nm−640nm band-pass. To generate reliable TGL detection data, a pulse detection threshold of 0.5 volts was set through the work reported in this paper.

In order to generate statistically valid histogram data, a high concentration of europium beads (~30,000 beads per 1mL) was used. The arrival rate of target beads was calculated from the sample flow rate (~ 100 μL per min) to be approximately 50 beads per second. Figure 4B and C show the real-time counting results for one minute with 3,265 TGL events counted: Figure 4B shows the TGL events temporal location, and each "+" marker represented the signal pulse height (Y-axis; volts) and arrival time (X-axis; μs) when a TGL event passed the interrogation region of TGL flow cytometer; while Figure 4C shows the statistical counting histogram for the signal pulses above 0.5 volts.

Thanks to the new europium calibration beads and new UV LED excitation (15mW peak power in contrast to 7mW in the previous report), most of the TGL pulses were clearly resolved from the background level (0.3volts), and the highest TGL signal pulse was 8.2 volts (the calculated maximum signal-to-background ratio was up to 27). In contrast to our previously reported results [14], the improvements in new calibration beads [minimum aggregation after ultrasonication and comparatively low coefficient of variation (CV) of 27.8% in luminescence intensity] led the experimental data to more closely fit the theoretical concepts predicted[13]: 81% of TGL target beads registered into higher channels (>2 volts) and the peak channel of around 6.3 volts (62% populated from 4.5volts to 8.2 volts). We believe only two factors contribute to form such a profile of TGL flow counting histogram: the peak population at higher channels (>4.5volts) reflected the europium calibration beads were exposed to maximum excitation (exposed to UV LED excitation for 100μs); while the long "tail" towards lower channels was either due to partial excitation of europium beads by UV LED pulses [some beads may entered the excitation region some time after the 100μs UV pulse initiation, and some other beads may exited the excitation zone some time before the 100μs UV pulse completion[13]], or due to the inhomegeneity of the volume and/or loading of the calibration beads. According to the histogram population trend (< 2volts), the height of some TGL signal pulses (>75 events in the channel 0.5volts and >75 events in the channel 0.4volts) was below 0.5 volts but still above the background level (0.3volts), which fact (further 5% undetected events below 0.5volts) should be taken into the consideration when it comes to analysing the counting efficiency by TGL flow cytometer. The undetected events could become detectable when excitation efficiency of the optics (8% for the current development) of LED excited TGL flow cytometer is improved.

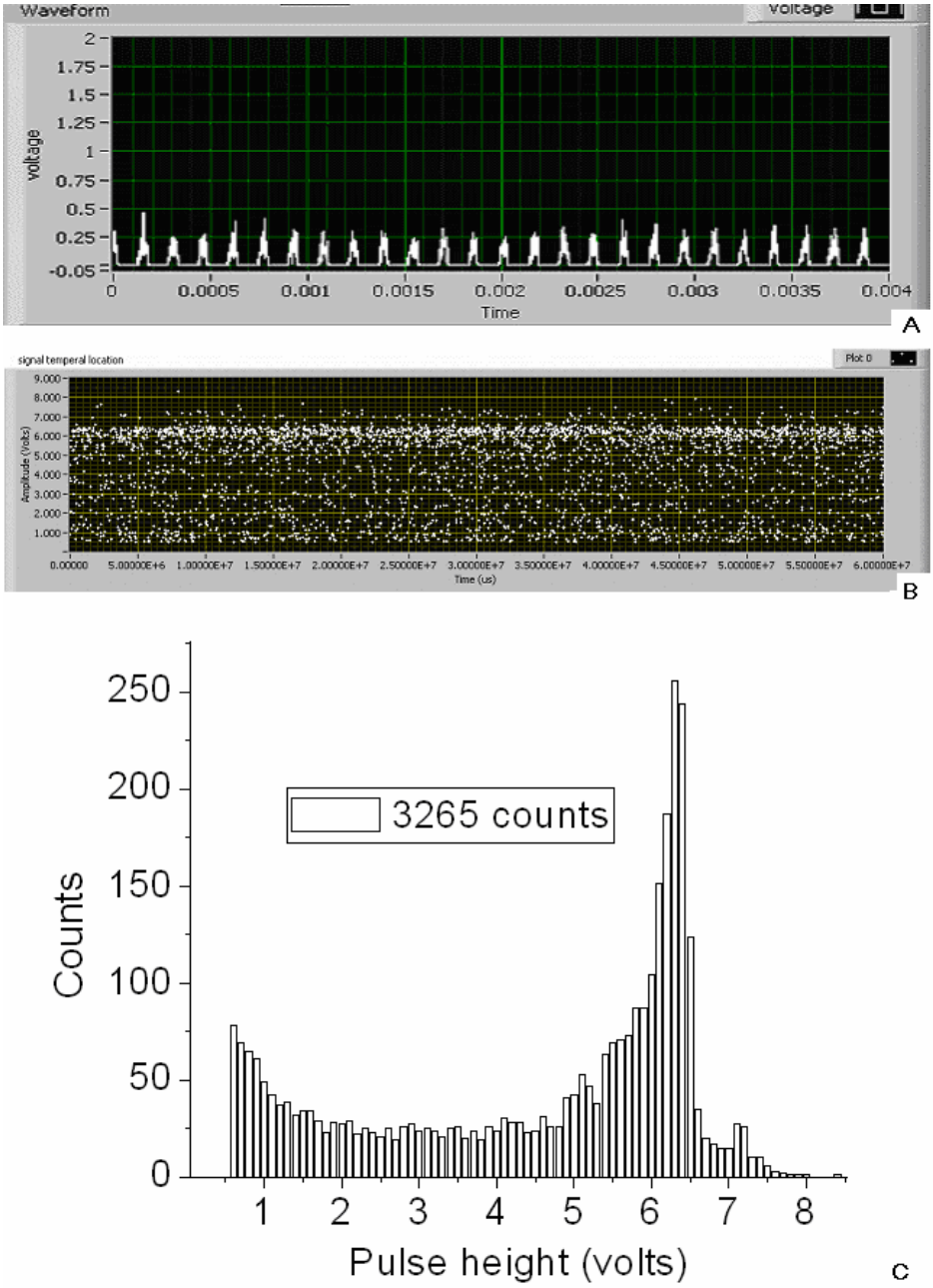

Figure 4 Real-time counting europium calibration beads by UV LED excited TGL flow cytometer: A). a 4-millisecond section of the TGL flow cytometer pulse train during a quiescent period where no particles were present. The minima and peaks indicate that the CPMT was respectively in the off and on states. The TGL flow counting background level was less than 0.3 volts when there was no TGL event present in the time-gated detection periods; B). TGL events temporal location, each "+" marker represents the signal pulse height (volts) and arrival time (μs) when a TGL event passed the interrogation region of TGL flow cytometer; C). The statistical counting histogram for the signal pulses above 0.5 volts. The counts shown on the left below 3 Volts are the result of the particle being in the illumination zone during the dark period between LED pulses and exposed for less than 100 μs from UV pulses.

Recovery rates for rare-event counting of beads

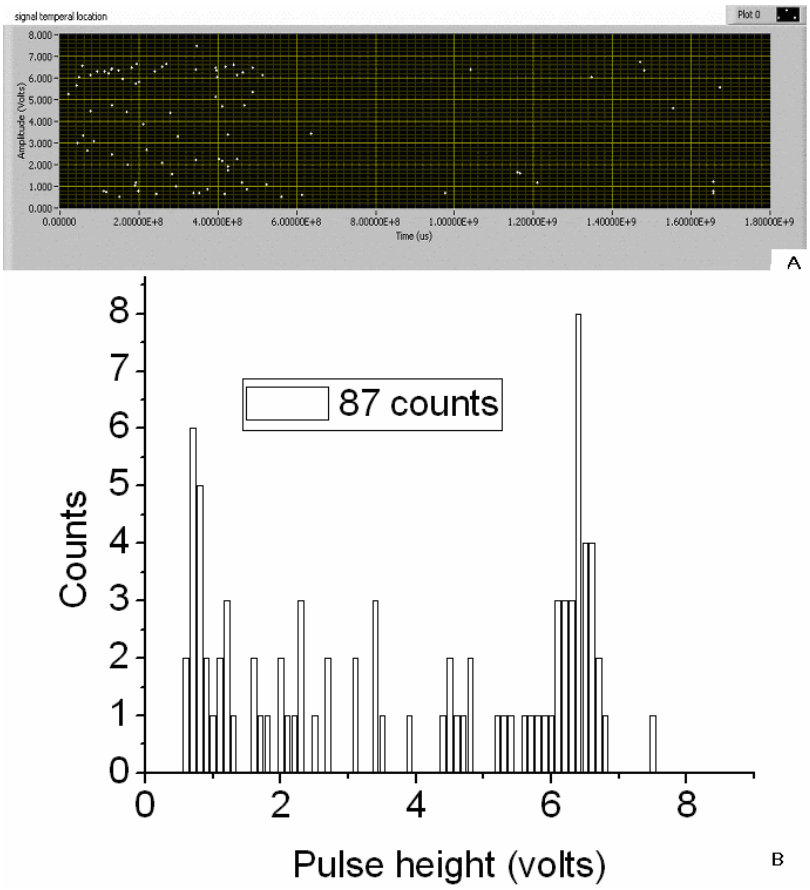

Figure 5 Recovery of 97±1 beads (Sample No.1) using TGL flow cytometer resulting in 87 beads counted: A). temporal location of TGL events; B). TGL flow cytometer counting histogram

There were 3 samples containing ~100-sorted beads each tested by TGL flow cytometer resulting in 87, 91 and 85 events detected respectively. Figure 5 presents one of the typical results (sample No.1). Due to the fact that some target beads will stick to both the sample tube and the injection needle of flow cell, a number of dilution-washing-mixing steps were involved during the rare-event recovery experiments in this paper. The original sorted beads samples were diluted into ~800µl, which resulted in the majority of beads populated in the first ~8 minutes (Figure 6A); without pausing the TGL flow cytometer, the sample tube was then washed by adding 800µl MABB buffer and vortex mixing, continuing to be counted, followed by a further wash of 400µl water; the whole counting was terminated by the time of 30 minutes (1.8×10^9µs). Figure 6B statistically presented the TGL flow cytometer counting histogram with 87 events counted. Due to the low number of target beads, the histogram profile was not so clear to appear consistent to that 3265 counting result (in the preceding subsection), however, the peak channel was still quite clearly populated around 6.4volts. According to the microscopy confirmation (97±1 counts) on the exact number of beads each sample contained, the recovery rate for rare-event counting of ~100-bead sample was calculated as 91%±3% [(87+91+85)/(97*3)=91%].

There were 6 samples containing ~10-sorted beads; each was tested with the TGL flow cytometer resulting in 12, 10, 10, 11, 9 and 11 events detected respectively. Figure 6 presents one of the typical results (sample No.3). The original sorted beads samples (~100µl) were tested directly without dilution, resulted in the

majority (6 counts for sample No.3, sometimes 9 counts in other samples) of beads populated in the first ~1 minutes (data not shown); without pausing the TGL flow cytometer, the sample tube was then washed by adding ~600μl water and vortex mixing, continuing to be counted; the whole counting was terminated by the time of 8 minutes (5×10^8μs). Figure 6 statistically presented the TGL flow cytometer counting histogram with 11 events counted. According to the microscopy confirmation (10±1 counts) on the exact number of beads each sample contained, the recovery rate for rare-event counting of ~10-bead sample was calculated as 100%±20% [(12+10+10+11+9+11)/10*6=100%].

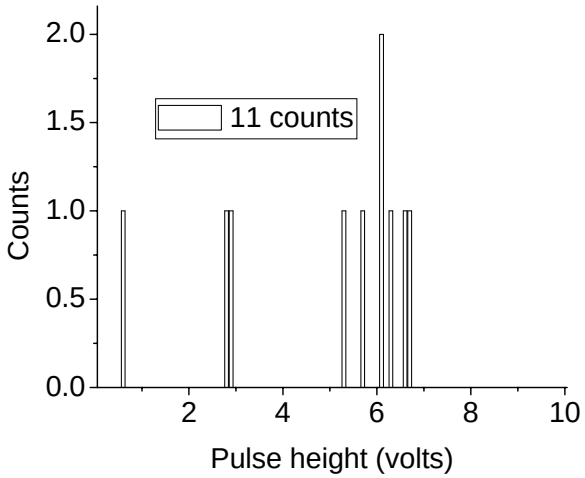

Figure 6 Recovery of 10±1 beads (Sample No.3) using TGL flow cytometer resulting in 11 beads counted.

TGL detection of rare-event beads from environmental water samples

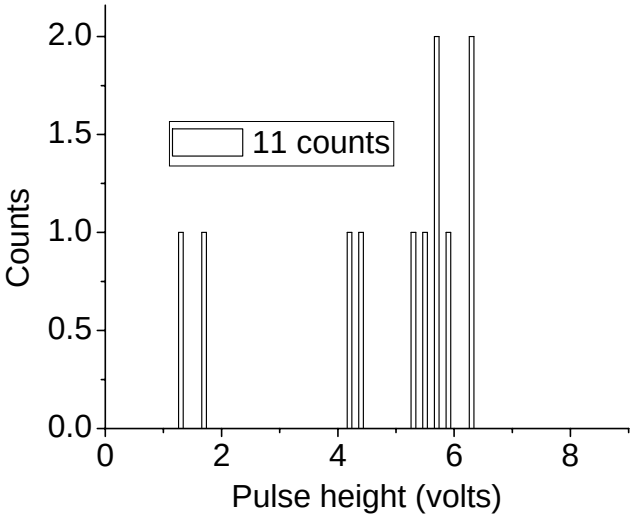

Figure 7 Recovery of 10±1 beads (Sample No.4) from water mud using TGL flow cytometer resulting in 11 beads counted.

The six 10-bead samples were spiked into 200μl water contaminate concentrates (mud) to further

approve the rare-event counting capability offered by the TGL flow cytometry technique, which resulted in 13, 11, 9, 11, 9, and 8 events detected respectively. The water concentrates did not increase the background level during the time-gated detection phase. Figure 7 presents one of the typical results (sample No.4). The beads samples containing mud background particles (~300μl) were tested directly without dilution, resulted in 9 counts appeared in the first ~3 minutes (figure of event temporal location was not shown); without pausing the TGL flow cytometer, the sample tube was then washed by adding ~400μl water and vortex mixing, continuing to be counted; the whole counting was terminated by the time of 8 minutes (5×10^8μs). Figure 7 statistically presented the TGL flow cytometer counting histogram with 11 events counted. The recovery rate for rare-event counting of ~10-bead sample against water mud background particles was calculated as 100%±30% [(13+11+9+11+9+8)/10*6=100%].

DISCUSSION AND CONCLUSION

Our new technique on TGL detection in flow cytometry has been evaluated to be successful in accurate recovery of a population of as small as 10 target μ-beads from other >1,000,000 background particles. The current development and evaluation of LED excited TGL flow cytometer for rare-event counting were essentially based on both the availability of new calibration beads and the accurate BD FACSAria^{TM} flow cytometer sorting to provide accurate/reliable number of rare-events in the test sample for evaluation. Another attraction of this technique is that it can use low-cost LED excitation. The excitation efficiency in current development of UV LED TGL flow cytometer was only ~8%, which limited further exploration using this device for detection of real biological agents. The optimum excitation wavelength to europium based chelates (probing luminescence dye) used in thus study is around 336nm. Other available europium complexes exist that have excitation maxima that match the emission of the UV LED. One of these is the europium Quantum Dye® with its TTFA enhancer[15,19] (TTFA is the mono-negative anion of thenoyltrifluoroacetone). The presence of excess complexes of $Gd(TTFA)_3$ in a micellar solution also can be used to increase the luminescence of the europium Quantum Dye [16,20]. Fortunately, there has been rapid progress since 2000 in UV LED commercial development (lead by Nichia, Japan) towards both shorter wavelengths and high peak powers, for example, 375nm LED in 2000, 365nm 2mW LED in 2002, 365nm 100mW LED in 2005 and 365nm 250mW in 2007 most recently. The costs of UV LED lasers has also decreased sufficiently that their use is commercially feasible.

References

1 A. L. Allan, S. A. Vantyghem, A. B. Tuck et al., Cytometry Part A **65A** (1), 4 (2005); E. A. Jones, A. English, S. E. Kinsey et al., Cytometry Part B-Clinical Cytometry **70B** (6), 391 (2006); K. Yamaguchi, K. Itoh, T. Masuda et al., Journal of Hepatology **45** (5), 681 (2006).

2 Howard M. Shapiro, *Practical flow cytometry*, fourth ed. (A John Wiley & Sons, INC., publication, 2002).

3 S. Bajaj, J. B. Welsh, R. C. Leif et al., Cytometry **39** (4), 285 (2000).

4 B. C. Ferrari and D. Veal, Cytometry Part A **51A** (2), 79 (2003).

5 D. S. Francy, O. D. Simmons, M. W. Ware et al., Applied and Environmental Microbiology **70** (7), 4118 (2004); W.-T. Liu and C. Lay., Clinics in Laboratory Medicine **7** (2), 65 (2007).

6 K. L. Johnson, H. Stroh, K. Khosrotehrani et al., Microscopy Research and Technique **70** (7), 585 (2007).

[7] D. A. Veal, D. Deere, B. Ferrari et al., Journal of Immunological Methods **243** (1-2), 191 (2000).
[8] G. Vesey, P. Hutton, A. Champion et al., Cytometry **16** (1), 1 (1994).
[9] P. Attfield, T. Gunasekera, A. Boyd et al., Australasian Biotechnology **9** (3), 159 (1999).
[10] T. S. Gunasekera, P. V. Attfield, and D. A. Veal, Applied and Environmental Microbiology **66** (3), 1228 (2000).
[11] B. C. Ferrari, K. Stoner, and P. L. Bergquist, Water Research **40** (3), 541 (2006); R. G. Mcclelland and A. C. Pinder, Journal of Applied Bacteriology **77** (4), 440 (1994).
[12] D. Deere, G. Vesey, N. Ashbolt et al., Letters in Applied Microbiology **27** (6), 352 (1998); G. Vesey, D. Deere, M. R. Gauci et al., Cytometry **29** (2), 147 (1997).
[13] D. Jin, R. Connally, and J. Piper, Cytometry Part A **71A** (10), 783 (2007).
[14] D. Jin, R. Connally, and J. Piper, Cytometry Part A **71A** (10), 797 (2007).
[15] R. C. Leif, L. M. Vallarino, M. C. Becker et al., Cytometry Part A **69A** (8), 940 (2006).
[16] R. C. Leif, M. C. Becker, A. Bromm Jr. et al., Proceedings of the SPIE - The International Society for Optical Engineering **6092**, 29 (2006).
[17] G. Vesey, J. S. Slade, M. Byrne et al., Journal of Applied Bacteriology **75** (1), 82 (1993).
[18] D. Jin, R. Connally, and J. Piper, Journal of Physics D-Applied Physics **39** (3), 461 (2006); R. Connally, D. Y. Jin, and J. Piper, Cytometry Part A **69A** (9), 1020 (2006).
[19] R. C. Leif, L. M. Vallarino, M. C. Becker et al., Cytometry Part A **69A** (8), 767 (2006).
[20] A. J. Bromm, Jr., R. C. Leif, J.R. Quagliano et al., Proceedings of the SPIE - The International Society for Optical Engineering **3604** (Optical Diagnostics of Living Cells II (Farkas DL, Leif RC, Tromberg BJ, editors).), 263 (1999); R. C. Leif, M. C. Becker, A. J. Bromm, Jr. et al., Proceedings of the SPIE - The International Society for Optical Engineering **4622**, 250 (2002).